Validity of Spatial Covariance Matrices over Time and Frequency

Ingo Viering[1)], Helmut Hofstetter[2)], Wolfgang Utschick [3)]

[1)]Siemens AG
Lise-Meitner-Straße 13
89081 Ulm, Germany
Ingo.Viering.GP@icn.siemens.de

[2)]Forschungszentrum
Telekommunikation Wien
Donau-City-Straße 1
1220 Vienna, Austria
hofstetter@ftw.at

[3)]Institute for Circuit Theory and Signal Processing
Munich University of Technology
Arcisstraße 21
80290 Munich, Germany
wout@nws.e-technik.tu-muenchen.de

Abstract-A MIMO channel measurement campaign with a moving mobile has been conducted in Vienna. The measured data will be used to investigate covariance matrices with respect to their dependence on time and frequency. This document focuses on the description of the evaluation techniques which will be applied to the measurement data in the future. The F-eigen-ratio is defined expressing the degradation due to out-dated covariance matrices. Illustrating the derived methods, first results based on the measured data are shown for a simple line-of-sight scenario.

I. Introduction

All mobile communication systems incorporating multiple antennas on one or on both sides of the transmission link strongly depend on the spatial structure of the mobile channel. Therefore, a lot of attention has to be paid to explore and to understand the spatial properties of the mobile channel.
Almost all multiple antenna algorithms, including beamforming, diversity as well as MIMO (multiple-input multiple-output) techniques are either directly or indirectly based on spatial covariance matrices and on their properties. A very important point is the stability over time. The longer the covariance matrices are constant, the longer the averaging interval can be chosen and the more reliable are the estimates derived from a covariance measurement.
A related aspect is the dependence of the covariance matrix on the frequency. Especially in frequency division duplex (FDD) systems, where uplink and downlink use different frequency bands, this is of special interest.
In order to obtain deeper insights, we will evaluate measurement data with respect to covariance matrices. A wideband MIMO channel sounder was used for the measurement campaign, which was carried out in Vienna last autumn with a moving mobile station.
This paper is focused on the description of the campaign and the derivation of the mechanisms for investigating the covariance matrices. Results for a simple line-of-sight (LOS) scenario are presented to illustrate the described methods. In [12] the techniques are applied to a large number of urban, rural and indoor scenarios.
Section I and II describe the equipment and the environment of the campaign. Section III derives the evaluation methods. We show how to extract the covariances from the data, we define a measure for the discrepancy of covariances called the *F-eigen-ratio* and we will review two different frequency transforms. These methods are applied to a simple LOS scenario of the measurement data in section IV. Finally, section V draws some conclusions.

II. Measurement Setup

The measurements were done with the MIMO capable wideband vector channel sounder RUSK-ATM, manufactured by MEDAV [1]. The sounder was specifically adapted to operate at a center frequency of 2GHz with an output power of 2 Watt. The transmitted signal is generated in frequency domain to ensure a pre-defined spectrum over 120 MHz bandwidth, and approximately a constant envelope over time. In the receiver the input signal is correlated with the transmitted pulse-shape in the frequency domain resulting in the specific transfer functions. Back-to-back calibration before each measurement enqured an unbiased estimate. Also, transmitter and receiver had to be synchronised via Rubidium clocks at either end for accurate frequency synchronism and a defined time-reference.
For studies on MIMO systems, the double-directional nature of the channel must be exploited. Therefore two simultaneously multiplexed antenna arrays have been used at transmitter and receiver.
At the mobile station, it is devised to cover the whole azimuthal range. To this end, a uniform circular array was developed by Fa. Krenn [2]. It is made of 15 monopoles mounted on a ground plane and was placed on top of a small trolley (Figure 1). The elements were spaced at 0.43λ (6.45cm) resulting in a diameter of around 30cm in the middle of the 90cm groundplane. Attention was paid on a height of the transmit antenna of about 1.5m above ground which fits the typical height of pedestrians using their phones. This also matches the COST259 [3] recommendations for mobile terminals.
The receiver was connected to a uniform linear array from T-

Fig. 1. Measurement setup at transmitter.

Fig. 2. Measurement setup at receiver.

NOVA, Germany. The antenna is made of eight patch elements spaced at a distance of $\lambda/2$ (7.5cm).
With above arrangement, consecutive sets of 15×8 transfer functions, cross-multiplexed in time, were measured every 21.5ms. Due to the nature of the channel sounder the acquisition period of one snapshot was limited to 3.2μs which corresponds to a maximum path length of about 1km.

III. Measurement Environment

The measurement data used for this paper was conducted during a measurement campaign in Vienna last autumn. For a first evaluation we took an Urban Area environment near the Vienna University of Technology. The receive antenna was mounted on top of one of the highest buildings in the surroundings, the so called *Freihaus* in about 30m height (Figure 2).

All streets within the coverage area of our equipment were measured. Therefore the trolley was moved at speeds of about 3km/h on the sidewalks. This results in a snapshot resolution of more than 8 snapshots per wavelength λ, or per doppler cycle, respectively.
The measurement data contains LOS scenarios as well as diffraction over rooftops and shadowing around corners. This work is restricted to a simple LOS scenario as is given in Fig. 3. In this case the transmitter moves along *Wiedner Hauptstraße* in the direction as is marked with an arrow. The receiver is on top of the building on the opposite side of the street.

IV. Evaluation Techniques

Most beamforming algorithms are based on the spatial covariance matrices $\mathbf{R} \in \mathcal{C}^{K_a \times K_a}$, which contain information about the correlations of the K_a antenna signals. Let $\vec{x}(t)$ be the $K_a \times 1$ antenna signal vector. The signal covariance matrix is defined as

$$\mathbf{R} = \mathbf{E}\left\{\vec{x}(t) \cdot \vec{x}(t)^H\right\}. \tag{1}$$

Fig. 3. Map of the Measurement Route

In rich scattering environments and with large element spacings, its structure approaches the identity, whereas in highly correlated scenarios, e.g. with a present line-of-sight, it is getting more and more singular. Hence, it represents the spatial properties of the scenario from the signal processing point of view.
For the wide sense stationarity (WSS) assumption, second order statistics such as the covariance are constant within a certain time interval. However, a varying environment of course changes the covariance.
In addition, the covariance depends on the carrier frequency, since the visible array topology relates to the wavelength.
In this section, we derive, how we will investigate the time and frequency dependency in section V by help of the sounding measurements.

A. Extraction of Covariances

As already mentioned, the data is available as transfer functions. In the sequel, we will consider the covariance matrices at the base station. First, we extract a 5MHz band of the total band width of 120MHz around the center frequency f_c and transform the transfer functions to the time domain. The 5MHz is a typical bandwidth for third generation systems, e.g. UTRA FDD and UTRA TDD [4]. Starting at a certain time t_0 we set up the covariance matrix by averaging over all values of all impulse responses within a time interval Δt_{avg}, which should not be too long in order to ensure that WSS holds. Since we consider the covariance matrix at the base station, we can use the different mobile antennas to increase the number of available snapshots to achieve a better estimate.
We eliminate the noise contributions by subtracting a noise covariance matrix which is derived from a separate noise measurement.
Finally, the matrices are corrected by a measured calibration matrix $\mathbf{C}$ in order to compensate for calibration errors due to different properties of the feeder cables etc.
The result is a covariance matrix $\mathbf{R}(t_0, f_c)$ which represents the spatial signature of the complete impulse response, i.e. of all channel taps, and which is valid for a certain time t_0 and for a certain carrier frequency f_c. Formally, it can be written as

$$\mathbf{R}(t_0, f_c) = \frac{1}{T_x \cdot \Delta_S} \cdot \tag{2}$$
$$\mathbf{C}^H \cdot \left[\sum_{k=1}^{T_x} \sum_{s=S_0}^{S_0+\Delta_S} \sum_{\tau=1}^{N_\tau} \vec{h}_k(s,\tau) \cdot \vec{h}_k(s,\tau)^H - \mathbf{R}_{nn}\right] \cdot \mathbf{C}$$

where T_x and N_τ is the number of Tx antennas and the number of delay values, $S_0, S_0{+}1, \ldots, S_0{+}\Delta_S$ are the snapshot numbers in the time interval $[t_0; t_0 + \Delta t_{avg}]$ and $\mathbf{R}_{nn}$ is the measured noise covariance matrix. The elements of $\vec{h}_k(s,\tau)$ are the τth

impulse response values from transmit antenna k to all receive antennas of snapshot s, which is the inverse fourier transform of the corresponding transfer function in the 5MHz frequency band around f_c.

B. Measure for Covariance Distance

In order to compare the extracted covariance matrices, we will now define a measure expressing the discrepancy between two covariance matrices. Since we consider the eigen structure of the covariances, this measure will be denoted the *F-eigen-ratio*.

We assume, that the actual environment is described by the unknown covariance matrix $\mathbf{R}$. Instead of the correct matrix, we have knowledge about another covariance $\hat{\mathbf{R}}$ measured in a different scenario, e.g. at another time instance or in another frequency band. If we process $\hat{\mathbf{R}}$ and apply the result in the environment $\mathbf{R}$, we will get a degradation.

Many beamforming techniques are based on the eigenvectors of the signal covariance matrix [5]. Other methods can be viewed as approximations of the eigen methods [6]. Therefore we introduce the eigenvalue decompositions

$$\hat{\mathbf{R}} = \hat{\mathbf{W}} \cdot \hat{\mathbf{\Lambda}} \cdot \hat{\mathbf{W}}^H \quad ; \quad \mathbf{R} = \mathbf{W} \cdot \mathbf{\Lambda} \cdot \mathbf{W}^H \tag{3}$$

where $\hat{\mathbf{W}}$ and $\mathbf{W}$ contain all eigenvectors, and $\hat{\mathbf{\Lambda}}$ and $\mathbf{\Lambda}$ are diagonal matrices with their entries being the corresponding eigenvalues of $\hat{\mathbf{R}}$ and $\mathbf{R}$. Without the loss of generality, we assume unitary matrices $\hat{\mathbf{W}}$ and $\mathbf{W}$.

We define the reduced versions $\hat{\mathbf{W}}_F, \mathbf{W}_F \in \mathcal{C}^{K_a \times F}$ of the matrices $\hat{\mathbf{W}}, \mathbf{W}$ to contain the eigenvectors corresponding to the F largest eigenvalues of the covariance matrices $\hat{\mathbf{R}}$ and $\mathbf{R}$, respectively.

$\mathbf{W}_F$ is used for a low-rank approximation of $\mathbf{R}$. Hence,

$$\mathbf{\Lambda}_F = \mathbf{W}_F^H \cdot \mathbf{R} \cdot \mathbf{W}_F \tag{4}$$

is a diagonal with the F largest eigenvalues as entries. If we use $\hat{\mathbf{W}}_F$ instead of $\mathbf{W}_F$ for the low-rank approximation of $\mathbf{R}$, we get

$$\mathbf{R}_{\hat{\mathbf{W}}_F} = \hat{\mathbf{W}}_F^H \cdot \mathbf{R} \cdot \hat{\mathbf{W}}_F \tag{5}$$

which in general is not a diagonal. The traces of the matrices $\mathbf{\Lambda}_F$ and $\mathbf{R}_{\hat{\mathbf{W}}_F}$ are a measure for the collected power applying the low-rank transforms $\mathbf{W}$ and $\hat{\mathbf{W}}$. Hence, the quotient of the traces gives us some knowledge about the power loss in the case of having $\hat{\mathbf{R}}$ available only. The F-eigen-ratio is defined as

$$q_{eigen}^{(F)} = \frac{\mathrm{tr}\left\{\mathbf{R}_{\hat{\mathbf{W}}_F}\right\}}{\mathrm{tr}\left\{\mathbf{\Lambda}_F\right\}} = \frac{\sum_{k=1}^{K_a}\sum_{f=1}^{F} \lambda_k \cdot \left|\vec{w}_k^H \cdot \hat{\vec{w}}_f\right|^2}{\sum_{f=1}^{F} \lambda_k} \tag{6}$$

with the properties $0 \leq q_{eigen}^{(F)} \leq 1$ and $q_{eigen}^{(K_a)} = 1$. The second form is the element notation, where $\vec{w}_k$, $\hat{\vec{w}}_f$ and λ_k are the columns and diagonals of $\mathbf{W}_F$, $\hat{\mathbf{W}}_F$ and $\mathbf{\Lambda}_F$, respectively. The term $|\vec{w}_k^H \cdot \hat{\vec{w}}_f|^2$ accounts for the mismatch of both eigenbases.

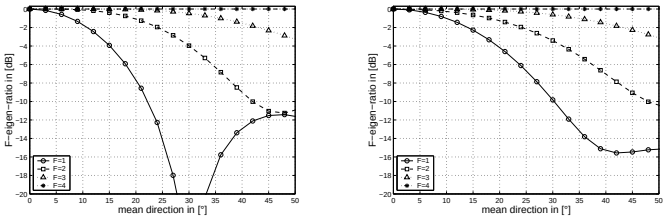

Fig. 4. F-eigen-ratio

The choice of the parameter F depends on the considered algorithm. In many downlink beamforming schemes, $F = 1$ is the only setting of interest, since usually a single beam is formed. More beams are not resolvable with a single receive antenna and therefore would interfere with each other. However, considering uplink scenarios or MIMO techniques, larger values might give more insights.

Figure 4 depicts $q_{eigen}^{(F)}$ using a 4-element uniform linear array (ULA) with $\lambda/2$ element spacing. The covariance matrices are computed theoretically by the expression

$$\mathbf{R} = \frac{1}{\Delta} \cdot \int_{\Theta-\Delta/2}^{\Theta+\Delta/2} \vec{a}(\vartheta) \cdot \vec{a}(\vartheta)^H d\vartheta \tag{7}$$

where Δ is the angular spread, which is assumed to be uniformly distributed here, Θ is the mean direction of arrival (DOA) and $\vec{a}(\vartheta)$ is the array response vector in the look direction ϑ. The integral is evaluated either analytically [7] or numerically.

The known covariance $\hat{\mathbf{R}}$ is determined by a mean DOA $\Theta = 0^o$ and two different spreads $\Delta = \{5^o, 30^o\}$, one in each plot. The abscissa represents the mean DOAs of the actual covariance $\mathbf{R}$ whereas the angular spread is constant in each plot. In the case of a mobile surrounding the base station, the abscissa would be proportional to a time axis. Note, that for a spread of $\Delta = 0^o$ and $F = 1$, the covariances are of rank 1 and the F-eigen-ratio is identical with the beam pattern.

The F-eigen-ratio gets higher with rising F values, since with a higher-rank approximation it is more likely to match the signal carrying dimensions. It is not a monotone function due to the sidelobes of the beampatterns corresponding to the eigenvectors in $\hat{\mathbf{W}}$. With a higher angular spread, the curves flatten out. However, the F-eigen-ratio is a sensible measure in the range down to approximately -12dB. These plots might be helpful to asses the measurement results in section V.

C. Frequency Transform

In Frequency Division Duplex (FDD) systems, up- and downlink experience different covariance matrices which complicates downlink beamforming techniques [8]. Various frequency transforms have been proposed in order to correct a

covariance matrix measured in the uplink for downlink application. We will focus on two algorithms which will be briefly described in the sequel. In section V we will apply both of them to the sounding measurements.

We assume an uplink and a downlink covariance matrix $\mathbf{R}_{ul}$ and $\mathbf{R}_{dl}$, respectively. Furthermore, we define the discrete up- and downlink array manifold $\mathbf{A}_{ul}, \mathbf{A}_{dl} \in \mathcal{C}^{K_a \times L}$ containing the L array response vectors $\vec{a}_{ul}(\vartheta_l), \vec{a}_{dl}(\vartheta_l)$ as columns. The look directions $\vartheta_1, ..., \vartheta_L$ are usually chosen to be equally spaced within the considered sector.

Hugl et al. propose in [10] to estimate the azimuth power spectrum $P(\Theta)$ in the uplink using Capon's beamformer [11]:

$$P(\Theta_l) = \frac{1}{\vec{a}_{ul}(\Theta_l)^H \cdot \mathbf{R}_{ul}^{-1} \cdot \vec{a}_{ul}(\Theta_l)}. \tag{8}$$

The APS is assumed constant in up- and downlink and the estimated downlink covariance matrix becomes

$$\hat{\mathbf{R}}_{dl}^{(H)} = \frac{1}{L} \cdot \sum_{l=1}^{L} P(\Theta_l) = \cdot \vec{a}_{dl}(\Theta_l) \cdot \vec{a}_{dl}(\Theta_l)^H. \tag{9}$$

In [9], Aste et al. find a matrix $\mathbf{T}^H \in \mathcal{C}^{K_a \times K_a}$ that transforms the array manifolds, i.e. $\mathbf{A}_{dl} = \mathbf{T}^H \cdot \mathbf{A}_{ul}$. The solution in a least squares sense is

$$\mathbf{T}^H = (\mathbf{A}_{ul} \cdot \mathbf{A}_{ul}^H)^{-1} \cdot \mathbf{A}_{ul} \cdot \mathbf{A}_{dl}^H. \tag{10}$$

Consequently, the downlink covariance estimate is written as

$$\hat{\mathbf{R}}_{dl}^{(A)} = \mathbf{T}^H \cdot \hat{\mathbf{R}}_{ul} \cdot \mathbf{T}. \tag{11}$$

In figure 5 the uplink is centered around $f_{ul} = 1905\text{MHz}$. The downlink frequency is varied between $1905\text{MHz} < f_{dl} < 2095\text{MHz}$. This relates to the UTRA FDD standard [4] where we have a duplex gap of 195MHz and uplink and downlink being centered around 2000MHz. At the latter frequency, the employed 8-element ULA has a $\lambda/2$ element spacing. The mean DOA is $\Theta = 30^o$ and the spreads are $\Delta = \{5^o, 30^o\}$ as in figure 4. The correct covariance $\mathbf{R}(f_{dl})$ at center frequency f_{dl} is compared with the untransformed $\mathbf{R}(f_{ul})$, with Hugl's approach $\hat{\mathbf{R}}^{(H)}(f_{dl})$ in (9) and with Aste's approach $\hat{\mathbf{R}}^{(A)}(f_{dl})$ in (11). The plots show the F-eigen-ratio $q_{eigen}^{(F)}$ derived in the previous section for $F = 1$ (solid lines) and $F = 2$ (dashed lines), where all covariance matrices are computed according to (7).

The maximal F-eigen-ratio is $\approx -0.5\text{dB}$ which does not seem too serious. For a moderate angular spread, Hugl's transform eliminates the error. With larger angular spreads, a bias occurs, since Hugl's transform is not self-reproducing, i.e. $\mathbf{R}(f_{ul}) \neq \hat{\mathbf{R}}^{(H)}(f_{ul})$. An interesting point is, that it seems to be almost independent of the duplex gap.

Aste's transform performs slightly better in the depicted range for the higher angular spread. However, the differences in the range of $0\text{dB} - 0.2\text{dB}$ will vanish, if any real world effects are taken into account.

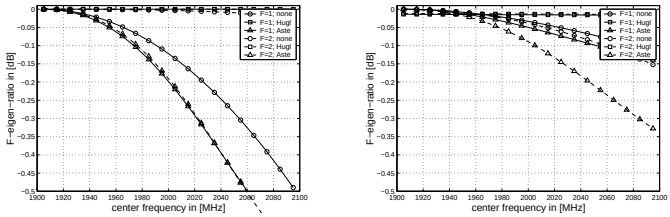

Fig. 5. Comparison of Frequency Transforms

A further aspect to mention is, that the F-eigen-ratio for $F = 2$ is smaller than for $F = 1$ in the right plot. Obviously, the sensitivity of the defined F-eigen-ratio $q_{eigen}^{(F)}$ on a frequency shift increases both with the considered rank F and the angular spread, respectively. Furthermore, note that the F-eigen-ratio is a relative measure and thus $q_{eigen}^{(2)} < q_{eigen}^{(1)}$ is not applicable for the corresponding receiver powers for $F = 1$ or $F = 2$.

V. Results

In the previous section, we described the mechanisms for evaluating measurement data. Now, we will show first results where we applied these techniques to the sounding measurement. Statistical results for a large number of urban, rural and indoor environments are given in [12].

The considered environment is a simple line-of-sight (LOS) scenario, where we walked along the street at the bottom of the "Freihaus" building (cf. figure 3).

The covariance matrices are computed according to (2). They are averaged in a window of $\Delta_s = 200$ snapshots, which is equivalent to $\Delta t_{avg} = 4.3$sec. The covered distance during that interval is in the range of $20\lambda = 3$m. The WSS assumption is supposed to hold in this case. In other words, the covariances are averaged over ≈ 20 cycles of the maximum doppler frequency.

In figure 6 a 5MHz band around the center frequency $f_{c0} = 1997.5\text{MHz}$ is extracted from the total bandwidth of 120MHz around 2000MHz. The covariance matrices $\mathbf{R}(t_0, f_{c0})$ are set up for different starting positions t_0 of the temporal averaging window. $\mathbf{R}(0, f_{c0})$ is the "known" environment. The left plot in figure 6 depicts the F-eigen-ratio versus t_0 for $F = 1$ and $F = 2$.

The F-eigen-ratio remains constant over a relatively long period of ≈ 30sec. Then it drops rapidly. The reason for this steep

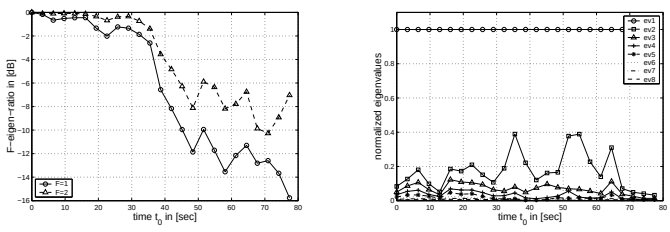

Fig. 6. F-eigen-ratio and Eigenvalues versus Time

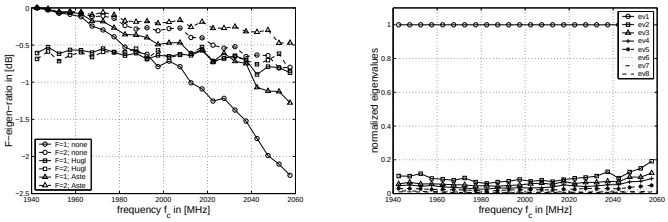

Fig. 7. F-eigen-ratio and Eigenvalues versus Frequency

slope is twofold. First, the mobile runs out of the beam formed at $t_0 = 0$ and second the angular velocity increases due to the small distance between the mobile and the base station. As in figure 4 the $F = 2$ curve is above the $F = 1$ curve.

The right plot of figure 6 shows the corresponding eigenvalues of the "unknown" covariance matrices $\mathbf{R}(t_0, f_{c0})$, where the eigenvalues are sorted and the strongest is normalized to 1 in each covariance matrix. That is, we do not see any short-term or long-term amplitude fluctuations in these plots.

We observe that the smallest eigenvalues are close to zero. This indicates that the noise elimination, i.e. the subtraction of the noise covariance matrix was correct. The second eigenvalue at $t_0 = 0$ is already very low, which justifies that we did not consider the cases $F > 2$.

Note, we do not completely compensate for the short-term effects (fast fading) by averaging over 20 fading periods which causes the zick-zack in the plots.

In figure 7 the covariance matrices $\mathbf{R}(t_0, f_c)$ are set up for $t_0 = 0$ and different center frequencies f_c. The "known" covariance matrix is $\mathbf{R}(0, 1942.5\text{MHz})$, i.e. at the lowest band of the available bandwidth. This is chosen, since in FDD systems, the uplink is usually positioned in the lower frequency band due to less attenuation. The frequency dependence of the F-eigen-ratio is shown in the left plot of figure 7.

Qualitatively spoken, we observe similar effects as in figure 5. Aste's transform improves the performance over the complete range, whereas Hugl's transform shows a constant F-eigen-ratio over the depicted range including the bias discussed in section IV-C. The $F = 2$ curves (dashed style) run above the $F = 1$ curves (solid style) except in Hugl's case.

However, the F-eigen-ratio is much lower than in the theoretical plots in figure 5. With the maximum duplex gap of 115MHz, we have an F-eigen-ratio of less than -2dB compared with -0.5dB at a duplex gap of 190MHz in the theoretical plots. Two major reasons might be responsible for this degradation:

- The assumption, that the azimuth spectrum is constant over frequency does not hold in this scenario. This would introduce an additional variation to the covariances for both the untransformed and the transformed cases.
- The array calibration is imperfect. This would affect particularly the frequency transforms, since they change from the signal domain to the azimuth domain and back. The investigations of the untransformed covariances as well as of the temporal behavior are restricted to the signal domain, i.e. they are less sensible to calibration errors.

This aspect will be discussed in more detail in the future.

The corresponding eigenvalues of the "unknown" covariances $\mathbf{R}(0, f_c)$ are shown in the right plot of figure 7. Again we find all the eigenvalues except the first one at a very low level, which verifies the noise elimination.

VI. Conclusions

We presented first evaluations of a wideband MIMO measurement campaign done in Vienna. The focus of this document was on the description of the measurement setup and of new evaluation methods which will be used to analyze the measured data in future work.

We defined the F-eigen ratio which is a measure for the discrepancy of two covariance matrices. The task of this measure was illustrated by investigating the time and frequency dependence of theoretically computed covariance matrices. Two different frequency transforms were reviewed to reduce the frequency dependence.

Finally, the derived techniques were applied to the measured covariance matrices. A simple line-of-sight scenario was chosen. As in the theoretical results, the covariances were very stable over time. However, the degradation over frequency was significantly higher than in theory. This has to be discussed in more detail in future work.

Acknowledgments

The authors would like to thank T-Nova GmbH for supporting the receive array.

References

[1] R. Thomä, D. Hampicke, A. Richter, G. Sommerkorn, A. Schneider, U. Trautwein, W. Wirnitzer, "Identifi cation of Time-Variant Directional Mobile Radio Channels," *IEEE Trans. on Instrumentation and Measurement*, vol. 49, no. 2, pp. 357-364, April 2000.

[2] Walter Krenn, Hochfrequenztechnik GmbH. Am Kanal 27, 1112 Vienna, Austria.

[3] L. M. Correia (Editor), *WIRELESS FLEXIBLE PERSONALIZED COMMUNICATIONS*, fi nal report of COST Action 259, European Union, 2000.

[4] Specifi cation Home Page, *3rd Generation Partnership Project*, www.3GPP.org/specs/specs.htm

[5] C. Brunner, W. Utschick, J.A. Nossek, "Exploiting the short-term and long-term channel properties in space and time: eigenbeamforming concepts for the BS in WCDMA," *European Transactions on Telecommunications, Special Issue on Smart Antennas*, VOL. 5, 2001

[6] I. Viering, T. Frey, G. Schnabl, "Hybrid Beamforming: Eigen Beamforming on Beam Signals," *International Zurich Seminar on Broadband Communications*, Zurich, Swiss, February 2002

[7] J. Salz, J. H. Winters, "Effect of Fading Correlati on on Adaptive Arrays in Digital Wireless Communications," *IEEE International Conference on Communications ICC'93*, Geneva, Switzerland, pp. 1768-1774, 1993

[8] C. Brunner, J. Hammerschmidt, J.A. Nossek, A. Seeger, "Space-Time Eigenrake and Downlink Eigenbeamformer," *IEEE Globecom 00*, November 2000, San Francisco, USA

[9] T. Aste, P. Forster, L. Féty, S. Mayrargue, "Downlink Beamforming Avoiding DOA Estimation for Cellular Mobile Communications," *Proceedings of the International Conference on Acoustics, Speech and Signal Processing*, Seattle 1998

[10] K. Hugl, J. Laurila, E. Bonek, "Downlink Beamforming for Frequency Division Duplex Systems," *Proc. IEEE Globecom 99*, Rio de Janeiro, 1999

[11] J. Capon, "High-Resolution Frequency-Wavenumber Spectrum Analysis," *Proc. IEEE*, Vol. 57, no. 8, pp. 1408-1418, Aug. 1969

[12] I. Viering, H. Hofstetter, W. Utschick, "Spatial Long-Term Variation in Urban, Rural and Indoor Environments," *COST273 5th Meeting*, Lisboa, Portugal, September, 2002